International Journal of Nanomedicine

Dovepress
open access to scientific and medical research

Open Access Full Text Article

ORIGINAL RESEARCH

One-Step Synthesis of Polypyrrole-Coated Gold Nanoparticles for Use as a Photothermally Active Nano-System

This article was published in the following Dove Press journal:
International Journal of Nanomedicine

Maha Fadel[1]
Doaa Abdel Fadeel[1]
Moustafa Ibrahim[2]
Rania M Hathout[3]
Abdullah I El-Kholy[1]

[1]Department of Medical Applications of Laser, Pharmaceutical Technology Unit, National Institute of Laser Enhanced Sciences (NILES), Cairo University, Giza, Egypt; [2]Physics Department, Faculty of Science, Banha University, Banha, Egypt; [3]Department of Pharmaceutics and Industrial Pharmacy, Faculty of Pharmacy, Ain Shams University, Cairo, Egypt

Objective: This paper introduces a simple one-step and ultra-fast method for synthesis of highly photothermally active polypyrrole-coated gold nanoparticles. The synthesis process is so simple that the reaction is very fast without the need for any additives or complicated steps.

Methodology: Polypyrrole-coated gold nanoparticles (AuPpy NPs) were synthesized by reacting chloroauric acid ($HAuCl_4$) with pyrrole (monomer) in aqueous medium at room temperature. These nanoparticles were characterized by UV–visible–NIR spectrometry, transmission electron microscopy (TEM), AC conductivity, zeta sizer and were evaluated for dark cytotoxicity and photocytotoxicity using human hepatocellular carcinoma (HepG2) cell line as a model for cancer cells.

Results: The synthesized AuPpy NPs showed a peak characteristic for gold nanoparticles (530–600 nm, molar ratio dependent) and a wide absorption band along the visible–NIR region with intensity about triple or even quadruple that of polypyrrole synthesized by the conventional $FeCl_3$ method at the same concentration and under the same conditions. TEM imaging showed that the synthesized AuPpy NPs were composed of spherical or semi-spherical gold core(s) of about 4–10 nm coated with distinct layer(s) of polypyrrole seen either loosely or in clusters. Mean sizes of the synthesized nanoparticles range between ~25 and 220 nm (molar ratio dependent). Zeta potentials of the AuPpy NPs preparations indicate their good colloidal stability. AC conductivity values of AuPpy NPs highly surpass that of Ppy prepared by the conventional $FeCl_3$ method. AuPpy NPs were non-toxic even at high concentrations (up to 1000 μM pyrrole monomer equivalent) under dark conditions. Unlikely, light activated the photothermal activity of AuPpy NPs in a dose-dependent manner.

Conclusion: This method simply and successfully synthesized AuPpy NPs nanoparticles that represent a safe alternative photothermally active multifunctional tool instead of highly toxic and non-biodegradable gold nanorods.

Keywords: polypyrrole, gold nanoparticles, ultra-fast synthesis, AuPpy NPs, photothermal activity

Introduction

Polypyrrole belongs to a unique category of polymers known as the conducting polymers.[1] It is one of a series of heterocyclic polymers with attracting electrical properties; principally attributed to the delocalized π-bonded electrons over the polymeric backbone.[2,3] However, this π-conjugation in polypyrrole and other conducting polymers is also a major determinant for some of their unfavorable physical features such as insolubility and poor mechanical properties.[1,4] Polypyrroles could

Correspondence: Maha Fadel
National Institute of Laser Enhanced Sciences (NILES), Cairo University, Giza 12613, Egypt
Tel +20 1001649550
Fax +20 35 729499
Email mahafmali@hotmail.com

submit your manuscript | www.dovepress.com
DovePress
http://doi.org/10.2147/IJN.S250042

be synthesized by a variety of methods based on oxidative polymerization of the monomer (pyrrole). Oxidative polymerization may be induced chemically, electrochemically or via ultrasonic waves.[5–7] Despite drawbacks, the most traditional method for polypyrrole synthesis is the chemical oxidative polymerization of pyrrole using strong oxidants such as $K_2Cr_2O_7$ and metals in high oxidation states as $FeCl_3$ in the presence or absence of a dopant. Such methods are generally time-consuming and involve several steps.[8,9] Doping in conducting polymers is the process of incorporating a dopant into the polymer chain to alter its conducting properties. The dopant may be negatively charged (n-type) or positively charged (p-type) and incorporated via an oxidation (n-type) or a reduction (p-type) process.[1,10-12] Properties of polypyrroles depend on several factors such as the method of preparation, oxidants, additives and doping.[4] Recently, polypyrroles were introduced in medicine mainly as featured drug delivery systems, in biosensors and as templates for the regeneration of nervous pathways.[13–15] Photothermal therapy (PTT) is an approach depending on cell-death induction through hyperthermia. Concerning PTT, several techniques were established where the common factor is the use of a photothermally active material.[16] These techniques are applied either apart or in combination with others.[17,18] In this study, size-tunable and water highly dispersible polypyrrole-coated gold nanoparticles with high conductivity and high photothermal activity were synthesized in aqueous medium using chloroauric acid ($HAuCl_4$) as an oxidant in a simple one-step ultra-fast method. Synthesized polypyrrole-coated gold nanoparticles (AuPpy NPs) were characterized for morphology, size, AC electrical conductivity, zeta potential and then furtherly biologically studied as a photothermally active dual-purpose nano-system.

Materials and Methods

Chemicals and Reagents

Chloroauric acid ($HAuCl_4$), anhydrous ferric chloride ($FeCl_3$) and pyrrole were purchased from Sigma-Aldrich Corp. (St. Louis, MO, USA). Roswell Park Memorial Institute (RPMI) media, fetal bovine serum (FBS), trypsin-EDTA and streptomycin-penicillin G mixture were purchased from Lonza (Verviers, Belgium). 3-(4, 5-dimethylthiazol-2-yl)-2, 5-diphenyl tetrazolium bromide (MTT) was purchased from BIO BASIC CANADA (Ontario, Canada). All other reagents and solvents were of analytical grade.

Synthesis of Polypyrrole-Coated Gold Nanoparticles (AuPpy NPs) and Determination of Concentration

Preparation of Stock Solutions

A stock aqueous solution of 500 mM pre-distilled pyrrole, from which all pyrrole solutions were derived, was freshly prepared. Similarly, stock aqueous solution of 10 mM $HAuCl_4$ from which all $HAuCl_4$ solutions were derived, was freshly prepared.

Synthesis Procedure

One mL of $HAuCl_4$ (10mM) is added rapidly to 20 mL stirring aqueous pyrrole solution of concentrations 0.5 mM, 1 mM, 2.5 mM, 5 mM, 25 mM and 100 mM (representing 1:1, 1:2, 1:5. 1:10 1:50 and 1:200 molar ratios, respectively) at room temperature and the reaction is left for 1–2 mins. Several molar ratios were applied to detect the actual molar ratio of the reaction (complete reaction, no excess of either reactants) and to study the effect of monomer concentration on the nanoparticle sizes. The resulting solutions were centrifuged at 8000–30,000 rpm to get rid of byproducts and excess unreacted pyrrole. Supernatants were analyzed colorimetrically for unreacted pyrrole and/or $HAuCl_4$ concentrations to detect the actual molar ratio and pellets were re-dispersed in double distilled water (20 mL) to retain the original concentration. The concentration was determined in relation to pyrrole monomer equivalent (the concentration of pyrrole monomer undergoing polymerization upon the reaction). All preparations used for further characterization and study, unless otherwise stated, were synthesized via a reaction carried out at room temperature (i.e. 25°C). In order to understand the reaction in-depth, the reaction was carried out also both at 0°C and 100°C.

Synthesis of Polypyrrole by $FeCl_3$ (Conventional Method)

For comparison reasons, the polypyrrole polymer (Ppy*FeCl*$_3$) was synthesized using the conventional method via $FeCl_3$ as the chemical reagent. 600 µL of 500 mM pyrrole aqueous solution is added to 20 mL of 34.95 mM anhydrous $FeCl_3$ (MR: 2.33 $FeCl_3$: 1 pyrrole monomer, respectively) stirring aqueous solution at 25°C and the reaction was left for 20 minutes and further left for 2 hours to let completion of polymerization.[19,20] The resulting Ppy*FeCl*$_3$ was centrifuged at 500–1000 rpm then re-dispersed in 200 mL double distilled and sonicated

for 24–30 hours to obtain a homogenous suspension. The concentration was then adjusted to 10 mM by centrifugation/re-dispersion.

Characterization of the Synthesized Ppy$FeCl_3$ and AuPpy NPs Preparations

UV–Vis–NIR Spectrophotometry

UV–Vis–NIR spectra of all preparations were measured by a spectrophotometer (Rayleigh UV-2601, Beijing, China). All samples were diluted with the same dilution factor to facilitate comparison.

TEM Imaging

The morphology and size of AuPpy NPs and Ppy$FeCl_3$ were examined by a transmission electron microscope TEM (JEOL, Japan).

Zeta Potential and Particle Size Analysis

Zeta potentials, particle size and particle size distribution were measured on Malvern zetasizer (Malvern, UK).

Electrical Conductivity and Resistivity

AC electrical conductivity of the AuPpy NPs and free Ppy samples (Ppy$FeCl_3$) was measured using Precision LCR meter (GwInstek, LCR-8110G, Taiwan) at a frequency range of 20 Hz to 10 MHz.

The AC electric conductivity (σ) was calculated using the equation:

$$\sigma = \frac{d}{A} \times \frac{1}{R}$$

where (R) is the resistance measured at room temperature using two parallel platinum electrodes, fitted in a cylindrical glass tube, (A) is the area of the glass tube and (d) is the distance between electrodes.

In vitro Evaluation of Cytotoxicity and Photocytotoxicity

Cell Culture

Human liver carcinoma HepG2 cell line was selected as a cell line model to study the cytotoxicity. HepG2 cell line was purchased from the holding company for biological products and vaccines (VACSERA, Giza, Egypt). Cells were maintained at 37° C under a humidified 5% CO_2 atmosphere in RPMI medium containing 10% FBS and 1% penicillin-streptomycin antibiotic mixture (100 IU penicillin and 100 µg streptomycin).[21]

Cell Viability Test

MTT assay (3-(4, 5-dimethylthiazol-2-yl)-2, 5-diphenyl tetrazolium bromide assay) was performed to evaluate the viability of HepG2 cells[22] and the experiments were performed identically according to the procedure mentioned by Fadel et al[23] using 96-well plates but the incubation time was 24 hours only, using a primary stock solutions of 10 mM concentration (pyrrole monomer equivalent) diluted in growth media to reach the intended concentration. All experiments were carried out simultaneously and each experiment was repeated for at least three times.

Cytotoxicity and Photocytotoxicity

The dark cytotoxicity of the selected preparations was examined using serial concentrations of AuPpy and Ppy$FeCl_3$ aqueous suspensions (100 µM, 200 µM, 500 µM and 1000 µM, pyrrole monomer equivalent). Photocytotoxicity was assessed using the maximum safe concentration (the maximum concentration at which cell viability is nearly 100% in dark and above which the preparation begins to exert dark cytotoxicity; to exclusively investigate the effect of irradiation). For photocytotoxicity assessment, the test and the control wells were irradiated, after 24 hours of dark incubation, using white light of a halogen lamp (1W) for 10, 20 and 30 minutes. Cells were then re-incubated for 24 hours as a resting period and finally the MTT assay was applied.

Statistical Analysis

The data were statistically analyzed by two-way analysis of variance (ANOVA) test followed by Bonferroni multiple comparison test[24,25] using software, version 5.01. The differences were considered significant when the p-value is less than 0.05 and highly significant when the p-value is less than 0.01. The final data were expressed as means ± standard errors (SEs).

Results and Discussion

Synthesis of Polypyrrole-Coated Gold Nanoparticles (AuPpy NPs)

The synthesis reaction is based on the ability of Lewis acids to induce polymerization.[23,26] Chloroauric acid ($HAuCl_4$) is produced from the reaction between gold trichloride ($AuCl_3$); a strong Lewis acid [27] and hydrochloric acid (HCl).[28,29] Lewis acids are well known as initiators or co-initiators in many types of polymerization reactions

especially carbocation or cationic polymerization.[26] In such a reaction, chloroauric acid acts in a similar manner to Lewis acids (as $FeCl_3$); oxidizing pyrrole monomers into pyrrole radical cations.[30] But in contrast to Fe^{+++} ions which are converted into Fe^{++} upon reduction by pyrrole (i.e. oxidation of pyrrole),[31] Au^{+++} ions in $HAuCl_4$ are completely reduced into elemental gold Au^0 (zerovalent gold or gold atoms). Such a reaction is usually associated with and evidenced by the formation of gold nanoparticles (elemental gold).[32,33] Experimentally, as in most of radical polymerization reactions,[34] the actual molar ratio of the reaction between Au^{+++} and pyrrole is affected by several factors among which are temperature and concentration of both reactants. At 0°C and 25°C, for instance, the reaction molar ratio is around 1:2 $HAuCl_4$: Pyrrole, respectively while at 100°C, the reaction molar ratio becomes about 1:3 $HAuCl_4$: Pyrrole, respectively. This can be explained in the light of the reduction potentials of gold ions and oxidation potentials of pyrroles. At low temperatures, the reaction takes place relatively slower than that running at high temperatures.[34] So, at low temperatures, differences in the reduction potentials of gold (chloride) ions where $E°(AuCl_4^-/AuCl_4^-) < E°(AuCl_4^-/Au^0)$[35–37] drives polymerization in a multi-step reaction and gradual pyrrole oxidation/gold ion reduction takes place while at high temperatures, reduction potentials are not such critical due to the high energy of the reaction. In addition, high temperatures accelerate the reduction process leading to lacking of selectivity due to the thermodynamic instability of gold ions with respect to elemental gold.[38,39] Furthermore, $AuCl_4^-$ ions in aqueous solutions make equilibrium with $Au(OH)_4^-$ ions and high temperatures shift the equilibrium towards the formation of $Au(OH)_4^-$ decreasing the amount of reactive $AuCl_4^-$ available for reduction.[38] So, assuming constancy of pyrrole concentration, there will be a transient drop in the molar ratio (gold ions: pyrrole monomers) decreasing the competition between gold ions for pyrrole electrons and thus increasing the probability of complete reduction. According to Le Chatelier principle,[40–42] the continuous consumption of available $AuCl_4^-$ forces the equilibrium to the other side ($AuCl_4^-$ formation). Although this means that pyrrole reacts with less $AuCl_4^-$ ions per unit time, the reaction rate is almost not affected because at high temperatures, the time frame of the overall reaction becomes shorter.[38] This assumption is also confirmed by the flashing red color, characteristic for gold element nanoparticles, appearing in the reaction solution before turning black in case of high temperature reaction (gold nanoparticles are synthesized firstly prior to pyrrole polymerization or synonymously pyrrole radicals coupling). On the other side, at low temperature reactions (i.e. at 0 and 25°C), this flashing red color is completely absent as dark black color of polypyrrole appears firstly (polymerization begins before complete reduction of gold ions or at least occurs simultaneously). Mechanisms of pyrrole oxidative polymerization, following the oxidation of pyrrole monomers into pyrrole radical cations, are exclusively either radical-radical coupling or radical-monomer propagation (initiation/propagation/re-initiation/propagation … etc.).[30] The latter assumption, despite being chemically reasonable, is obviously less favorable here neither in case of pyrrole polymerization by $FeCl_3$ nor $HAuCl_4$. This is because if it was true; the reaction was to proceed till complete consumption of the monomer (living polymerization) or at least the reaction reachable molar ratio was to be much lower than that actually occurs[43,44] (Here, MR is about 2.33:1 in case of $FeCl_3$ and about 1:2 to 1:3 in case of $HAuCl_4$ oxidant: pyrrole, respectively) but on the contrary, the polymerization is ended early no matter how much the initiator/monomer molar ratio (I_0/M_0) was. This is an evidence that the first mechanism, where coupling between pyrrole radicals is dominant, is much favorable. At low temperatures, the suggested mechanism is that gold ions (Au^{+++}) are partially reduced to Au^{++} by pyrrole in the molar ratio (1:1), the produced pyrrole radical cations undergo coupling with the release of two protons. Then, the second step takes place where Au^{++} snatches another electron from either pyrrole monomer or dimer to be partially reduced into Au^+. Oxidation of pyrrole dimers by Au^{++} is favorable than pyrrole monomers due to the difference in oxidation potentials (pyrrole $E°$: +0.8 V, bipyrrole $E°$: +0.6 V).[45] The produced pyrrole and bipyrrole radical cations then undergo homogenous (pyrrole-pyrrole, bipyrrole-bipyrrole) or heterogenous (pyrrole-bipyrrole) coupling; resulting in the formation of dimers, trimers and tetramers. Finally, Au^+ ions are completely reduced into zerovalent gold Au^0 by oxidizing equal number of molecules (pyrrole monomers, dimers and/or oligomers). Since the oxidation potentials of pyrrole oligomers decrease linearly with increasing the number of pyrrole units,[46] the formed dimers and oligomers are more favorable to be oxidized than are pyrrole monomers. The typical resultant molar ratio according to this mechanism, neglecting other possible side reactions, is about 1:2 MR $HAuCl_4$: pyrrole, respectively (Figures 1 and 2). The use of serial molar

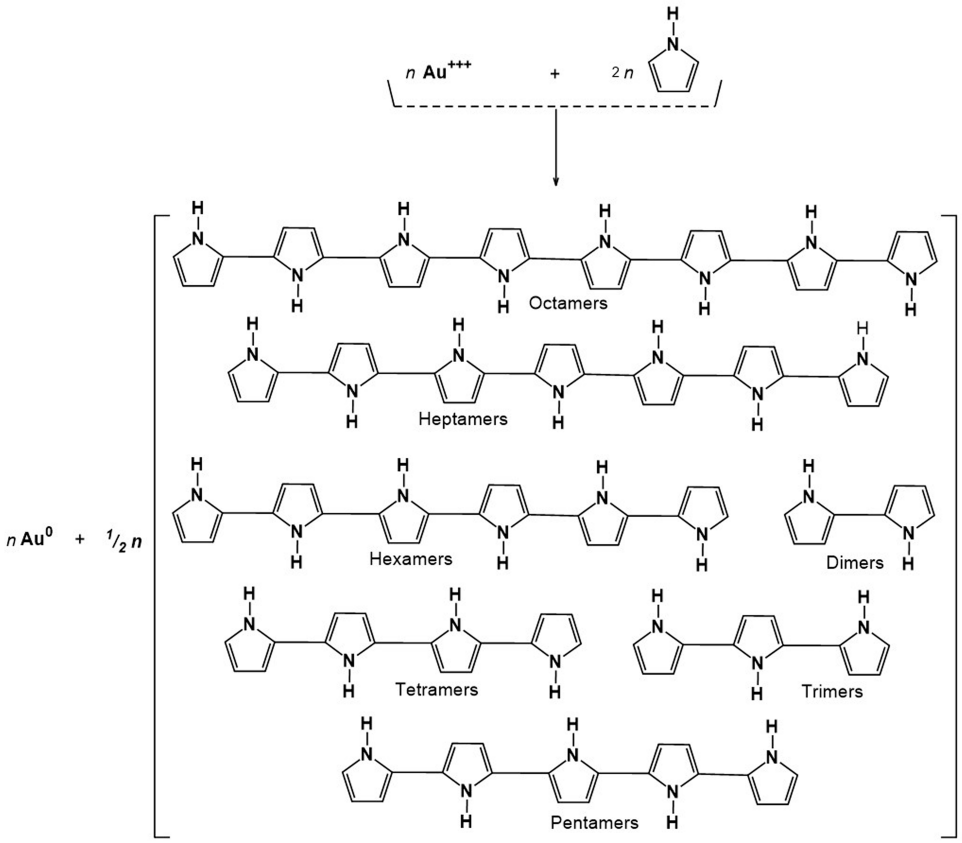

Figure 1 The resultant reaction between $HAuCl_4$ and pyrrole.

concentrations was to detect the reaction actual molar ratios and to study the effect of pyrrole monomer concentration on the properties of the synthesized particles.

Synthesis of Polypyrrole by $FeCl_3$ (Conventional Method)

The synthesized polypyrrole by the conventional method was in the form of amorphous black films precipitating from the aqueous solution during the reaction. After washing and centrifugation, dispersing process requires at least 24 hours on bath sonicator to get a well-dispersed homogenous suspension. The final suspension was greyish black to dark black color depending on concentration.

Characterization of the Synthesized Ppy$FeCl_3$ and AuPpy NPs Preparations

UV–Vis–NIR Spectrophotometry

Except for $AuPpy_{1:1}$, and Ppy$FeCl_3$, UV–Vis–NIR spectra showed a similar pattern of absorption between all AuPpy preparations with obvious differences in the visible and NIR regions (Figure 3). Other AuPpy suspensions showed a much higher absorption intensity than conventional Ppy$FeCl_3$ suspension (in the same concentration) especially in the visible and NIR region. It is also observed that the absorption intensity is inversely proportional to the particle size. This may explain why $AuPpy_{1:1}$ and Ppy$FeCl_3$ have the lowest absorption intensity among all preparations. The Au nanoparticles characteristic peak (visible region) and Ppy characteristic broad peak (NIR region) are overlapped and undistinguishable except for $AuPpy_{1:50}$ and $AuPpy_{1:200}$. This is because as the size of Au NPs clusters increases, the sharpness of the peak decreases and the peak is red-shifted making the peak undistinguishable from this of Ppy peak and vice versa.

TEM Imaging

TEM imaging of AuPpy suspensions shows gradual morphological and structural changes of particles as the molar ratio decreases (1:1 → 1:200). For high molar ratio (1:1 MR, atypical reaction); gold particles are seen as large bulk nano/microparticles either naked or coated with layer(s) of polypyrrole which in turn, is seen also as free shredded or torn films (Figure 4A). As the molar ratio decreases (i.e. 1:2 MR, complete reaction); polypyrrole-embedded clusters of

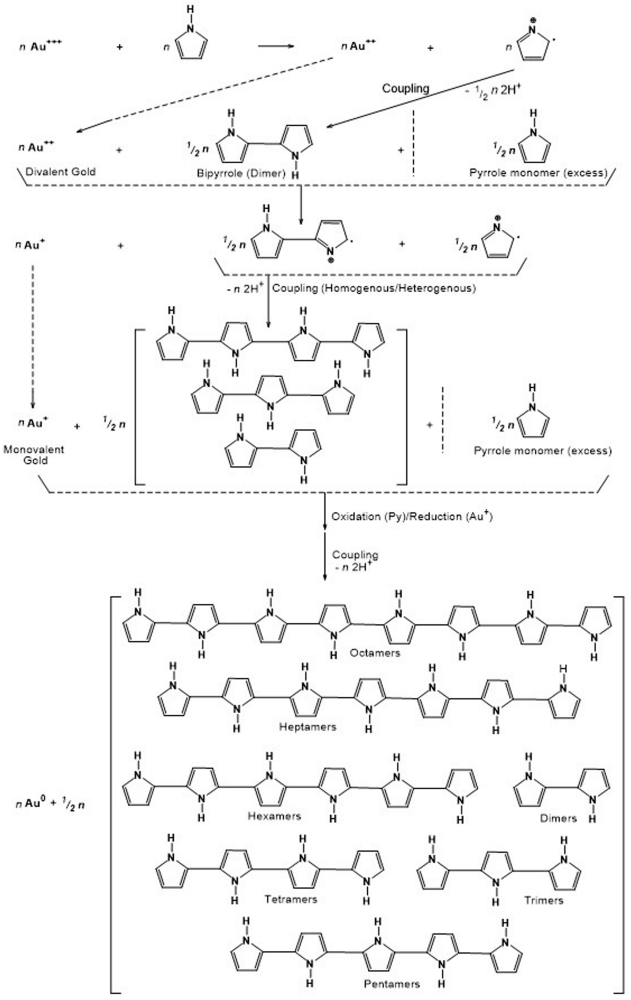

Figure 2 Mechanism of pyrrole oxidative polymerization by $HAuCl_4$.

spherical, semispherical and short rod-shaped gold nanoparticles appear as well as undifferentiated amorphic gold nano/microparticles with less free polypyrrole films than observed in 1:1 MR (Figure 4B). More differentiated polypyrrole-embedded gold nanoparticles clusters are observed by further decrease in molar ratio (1:5, 1:10, 1:50 and 1:200 MR) where the clusters sizes decrease with decreasing molar ratio until reaching nearly loose gold nanoparticles ($AuPpy_{1:200}$) and with almost the same size for the individual nanoparticles (~4–10 nm). Free polypyrrole films are almost absent (Figure. 4C–F). This behavior is somehow predicted. In case of high molar ratios (1:1 and 1:2 MR); gold nano-micro particles are nucleated in a medium of low-concentration pyrrole/polypyrrole. This leads to the formation of large and non-homogenous gold particles. This is a common well-known pattern concerning gold nanoparticles synthesis (size control by altering gold salt: reducing/capping agent molar ratio).[47–49] The formation of large particles (bulk gold particles) means that the total surface area of such particles will be much lesser than it would have been if the particles were smaller. In other words (supposing constancy of initial gold ions concentration); as the particle size of the synthesized gold particles increases, the total surface area of all particles decreases and vice versa. Assuming reaction completion, polymerized pyrrole quantity remains the same at all molar ratios (except for $AuPpy_{1:1}$ where the reaction is complete but total pyrrole is half the quantity in other AuPpy preparations). However, in case of low pyrrole concentration (i.e. 1:2 MR);

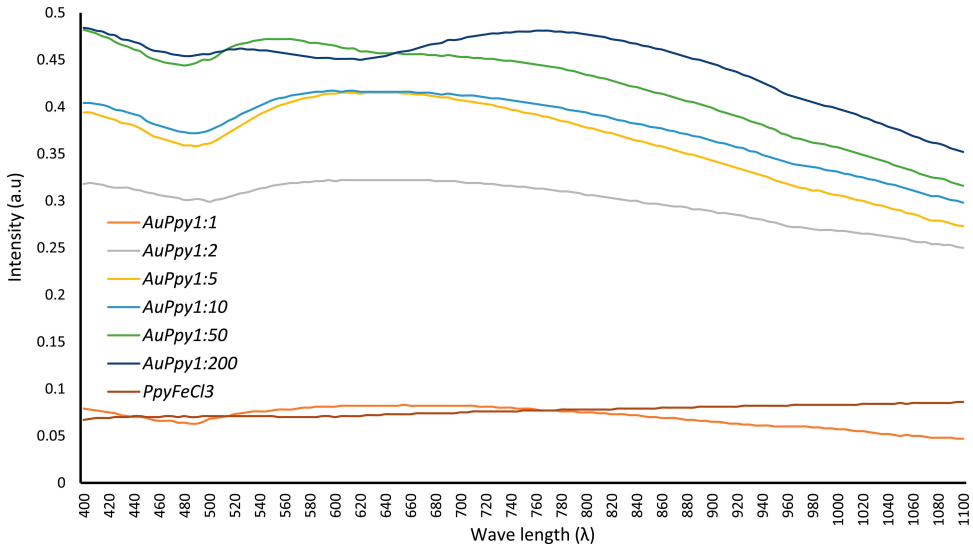

Figure 3 UV–Vis–NIR spectra of AuPpy and Ppy suspensions (Au is constant for all AuPpy preparations).

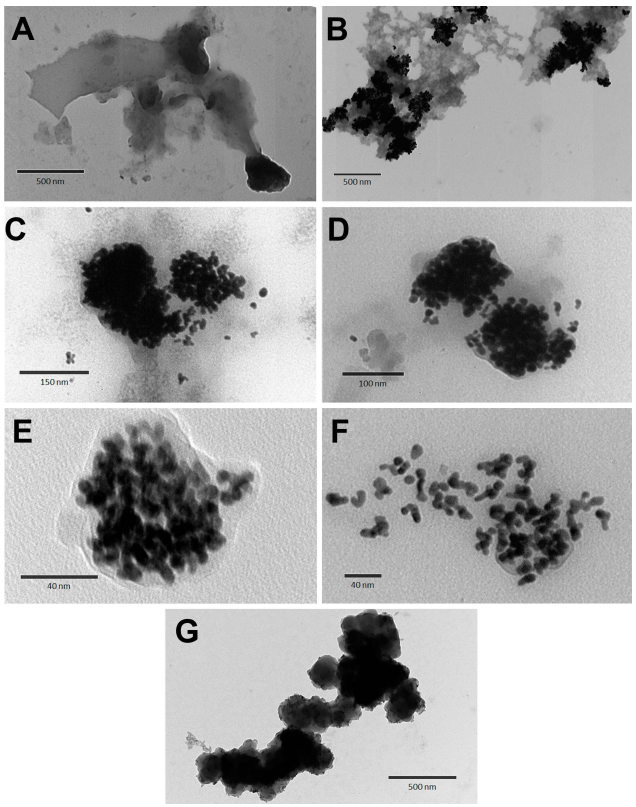

Figure 4 TEM imaging of (**A**) AuPpy$_{1:1}$, (**B**) AuPpy$_{1:2}$, (**C**) AuPpy$_{1:5}$, (**D**) AuPpy$_{1:10}$, (**E**) AuPpy$_{1:50}$, (**F**) AuPpy$_{1:200}$ and (**G**) Ppy*FeCl*$_3$.

the total area of the synthesized gold particles is too limited to assimilate all synthesized polypyrrole. As a result, excess polypyrrole remains free in the solution. On the other hand, the large total surface area accompanied with smaller gold nanoparticles enables them to adsorb most or all of synthesized polypyrrole. Assembly of the synthesized gold nanoparticles as polypyrrole-embedded clusters explains the broadening and red-shifting of the gold nanoparticles characteristic peaks in UV–visible spectra compared to loose traditional Turkevich gold nanoparticles.[50] This red-shifting and broadening is most announced in case of AuPpy$_{1:1}$, AuPpy$_{1:2}$ and AuPpy$_{1:5}$ where the clusters are the largest. Excepting AuPpy$_{1:1}$, and to less extent AuPpy$_{1:2,}$ all AuPpy preparations have almost the same intensity and the same pattern with overlapping and interference between Au nanoparticles and Ppy peaks. For AuPpy$_{1:200}$, the majority of gold nanoparticles are loose (no clusters) (Figure 4F), so gold nanoparticles peak is blue-shifted with less intensity (a behavior observed also for some polymer-conjugated small gold nanoparticles),[51] making it distinguishable from the broad peak of Ppy (at NIR region). This pattern is more announced in case of AuPpy$_{1:50}$ where the clusters are present but relatively smaller than those observed in AuPpy$_{1:1}$, AuPpy$_{1:2}$, AuPpy$_{1:5}$ and AuPpy$_{1:10}$. The presence of relatively small clusters (~55 nm in diameter) makes gold nanoparticles peak more distinguishable than in case of AuPpy$_{1:200}$ (more intensity). Ppy*FeCl*$_3$ appears under TEM imaging as undifferentiated amorphous nano/microparticles (Figure 4G). Despite being sonicated for a long time (~24–30 hours), the poor solubility of pure polypyrrole [52] seems to make particles aggregate together which reflects also on the stability of the suspension (rapid flocculation).

Zeta Potential and Particle Size Distribution

Except for AuPpy$_{1:1}$, all AuPpy Z-potentials have relatively high positive values with mean particle size ranging from ~25 nm to ~215 nm in coincidence with molar ratios. The negative Z-potential value in case of AuPpy$_{1:1}$ emphasizes the oddity of the 1:1 MR reaction in comparison with the rest 1:2 MR reactions where all Z-potential values are positive. Ppy*FeCl*$_3$ has a mean particle size of ~800 nm with a poor Z-potential value (−1.81 mV) (Table 1). Values of zeta potential reflect the high colloidal stability of AuPpy suspensions, except AuPpy$_{1:1}$, compared to Ppy*FeCl*$_3$ [53].

AC Conductivity

The data of AC conductivity curves show similar behavior in which they increase with increasing applied frequency from 20 Hz to 5 MHz (Figure 5).

AC conductivities for the AuPpy$_{1:1}$, AuPpy$_{1:2}$, AuPpy$_{1:5}$, AuPpy$_{1:10}$, AuPpy$_{1:50}$ and AuPpy$_{1:200}$ seem to be varying insignificantly. On the other hand, they show substantial increase in conductivity when compared with the Ppy*FeCl*$_3$ (about 1.25 x10^{-2} S.m^{-1} and 4x10^{-3} S.m^{-1} for AuPpy and Ppy*FeCl*$_3$samples respectively) at the

Table 1 Z-Potential and Z-Size Values of AuPpy and Ppy Preparations (Means ± SEs)

Formula	AuPpy 1:1	AuPpy 1:2	AuPpy 1:5	AuPpy 1:10	AuPpy 1:50	AuPpy 1:200	Ppy ($FeCl_3$)
Z-value Z-average size ± SD	−21 mV 215.9 ±171.5 nm	36.3 mV 165.5 ±108.1 nm	49.1 mV 147.1 ±45.31 nm	46.6 mV 90.06 ±39.29 nm	46.2 mV 56.64 ±30.02 nm	42.9 mV 25.06 ±9.6 nm	−1.81 mV 776.8 ±455.4 nm

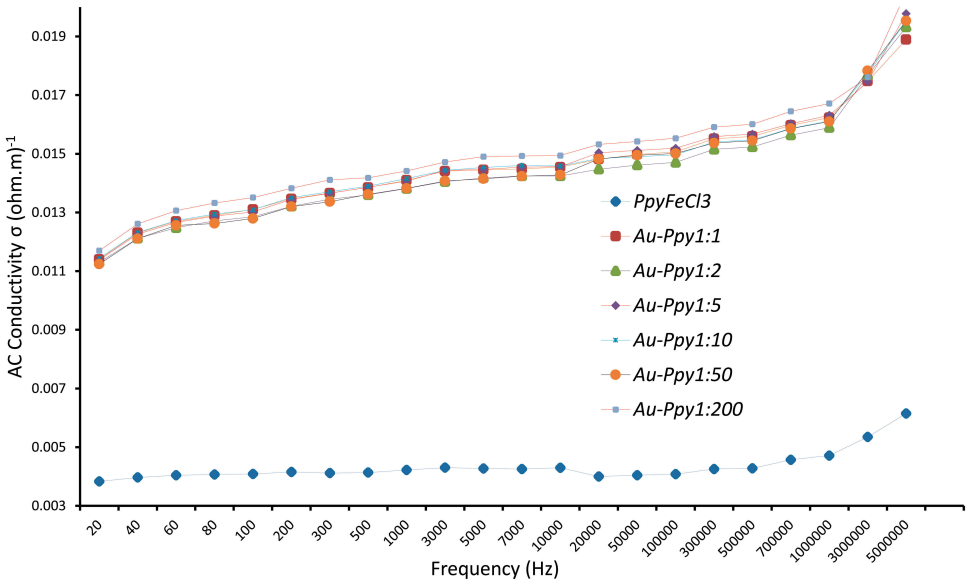

Figure 5 AC conductivity of AuPpy and Ppy.

applied frequency range. However, Ppy$FeCl_3$shows also a good conductivity but less than those of the AuPpy samples which signifies the influence of Au nanoparticles to improve the conductivity of the AuPpy suspensions.

Regarding that the measured samples were in the form of aqueous suspensions (not dry films) where conductivity doubtlessly falls, AC conductivity values are at the range of semiconductors and such a behavior is common for conductive polymers.[54] Generally, variations in particle size of the AuPpy samples do not reflect significant changes in conductivity because the actual molar ratio for all AuPpy preparations is the same (1Au:2Py, except for $AuPpy_{1:1}$). On the other size, the presence of gold nanoparticles highly improves the AC conductivity of AuPpy in comparison to conventional Ppy$FeCl_3$.

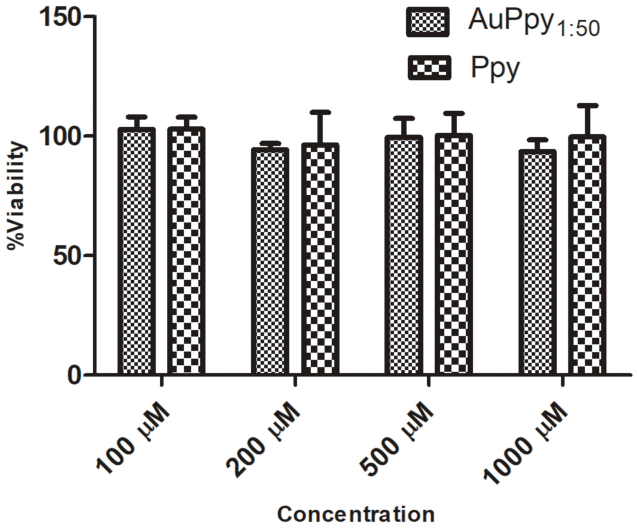

Figure 6 Dark cytotoxicity of $AuPpy_{1:50}$ and Ppy at different concentrations (Means ± SEs).

Cytotoxicity and Photocytotoxicity

Among all AuPpy preparations, $AuPpy_{1:50}$ was selected to study the dark cytotoxicity and the photocytotoxicity concerning several factors as particle size, stability and homogeneity. However, $AuPpy_{1:200}$ may be as good as $AuPpy_{1:50}$ but the very small particle size prevents full recovery of particles after centrifugation even under 30,000 rpm resulting in problems in calculating concentrations.

Both conventional Ppy (Ppy$FeCl_3$) and $AuPpy_{1:50}$ showed good cell tolerability up to 1000 µM under dark conditions (Figure 6). In contrast to Ppy, $AuPpy_{1:50}$ at 500 µM showed marked photocytotoxicity after 30 mins of irradiation (Figure 7A). Similarly, $AuPpy_{1:50}$ at 1000 µM exhibited high photocytotoxicity after 10 mins with no significant difference after extending the time of irradiation (Figure 7B). This could be attributed to heat absorption/dissipation rate. As the rate of heat absorption conquers the rate of heat dissipation, the resultant effect is temperature elevation and vice versa. When the temperature reaches critical level (i.e. ≥40°C), cells begin to lyse (i.e. cell death) and extent of lysis depends on the time of irradiation.

As mentioned before, the relatively higher electrical conductivity in case of AuPpy than Ppy results in higher photothermal activity. Another critical factor may be the

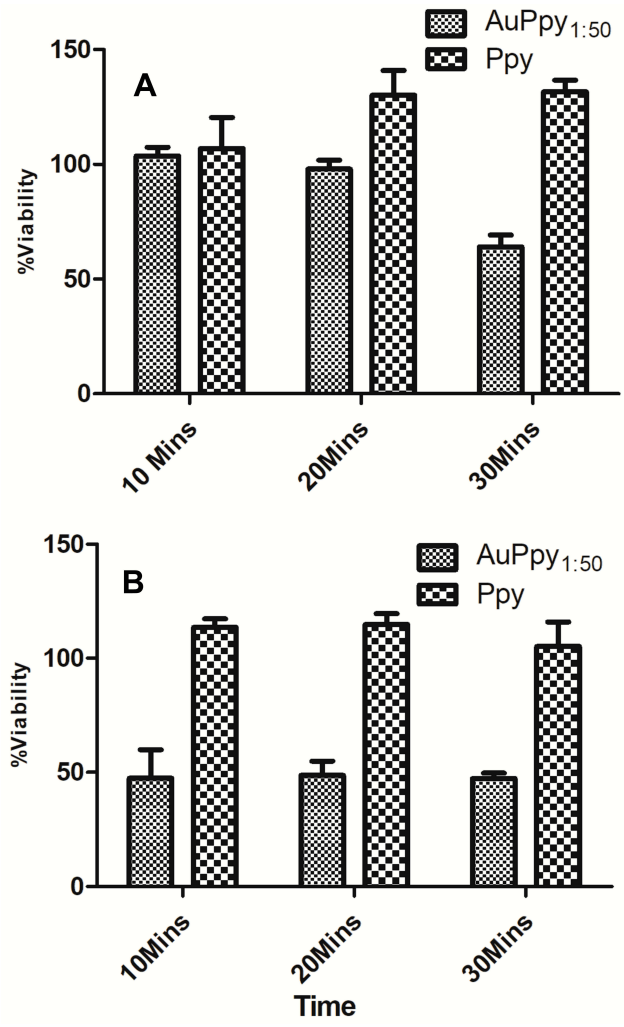

Figure 7 Photocytotoxicity of $AuPpy_{1:50}$ and Ppy at (**A**) 500 μM and (**B**) 1000 μM (Means ± SEs).

particle size where the very large particle size in case of conventional Ppy (~800 nm) limits its cellular uptake.

Conclusion

Polypyrrole-coated gold nanoparticles (AuPpy NPs) were synthesized simply and flexibly in various sizes and with photothermal activity much higher than the polypyrrole produced by the conventional chemical method in the same concentration and under the same conditions. Tunability and high water-dispersity of the synthesized AuPpy NPs represent additional advantages of the synthesis method. Besides, the synthesized AuPpy NPs were of good colloidal stability regarding both their physical stability and zeta potential values. This method enables optimum exploitation of the photothermal activity of polypyrrole by enhancing its water-dispersity and colloidal stability. The enhanced photothermal activity of the synthesized AuPpy NPs was confirmed by the in-vitro enhanced photo-cytotoxic activity on HepG2 cancer cell line. The synthesized nanoparticles can be utilized as a dual-purpose drug delivery system if loaded with an anticancer drug.

Disclosure

The authors declare no conflicts of interest in this work. This work is supported by a Cairo University project 2016 entitled: "Nano-systems in topical photodynamic therapy and photodynamic diagnosis: preparation, characterization and clinical evaluation".

References

1. Introduction of conducting polymers. In: Wan M, editor. *Conducting Polymers with Micro or Nanometer Structure*. Berlin, Heidelberg: Springer Berlin Heidelberg. 2008:1–15.
2. Stenger-Smith JD. Intrinsically electrically conducting polymers. Synthesis, characterization, and their applications. *Prog Polymer Sci*. 1998;23(1):57–79.
3. Skotheim TA. *Handbook of Conducting Polymers*. 2nd ed. Taylor & Francis; 1997.
4. Wang L-X, Li X-G, Yang Y-L. Preparation, properties and applications of polypyrroles. *React Func Polymers*. 2001;47(2):125–139. doi:10.1016/S1381-5148(00)00079-1
5. Bahraeian S, Abron K, Pourjafarian F, Majid RA. Study on synthesis of polypyrrole via chemical polymerization method. *Advan Mater Res*. 2013;795:707–710. doi:10.4028/www.scientific.net/AMR.795.707
6. Takakubo M. Electrochemical polymerization of pyrrole in aqueous solutions. *Synth Met*. 1986;16(2):167–172. doi:10.1016/0379-6779(86)90109-8
7. Kobayashi D, Sakamoto T, Matsumoto H, et al. Polypyrrole fine particle synthesis using ultrasound. *Kagaku Kogaku Ronbunshu*. 2015;41(2):153–156. doi:10.1252/kakoronbunshu.41.153
8. Della Pina C, Falletta E, Rossi M. *Sustainable Approaches for Polyaniline and Polypyrrole Synthesis*. Vol 12014.
9. Chitte HK, Shinde GN, Bhat NV, Walunj VE. Synthesis of polypyrrole using ferric chloride ($FeCl_3$</sub>) as oxidant together with some dopants for use in gas sensors. *J Sens Technol*. 2011;01(02):10. doi:10.4236/jst.2011.12007
10. Chen XL, Jenekhe SA. Bipolar conducting polymers: blends of p-Type polypyrrole and an n-Type ladder polymer. *Macromolecules*. 1997;30(6):1728–1733.
11. Ateh DD, Navsaria HA, Vadgama P. Polypyrrole-based conducting polymers and interactions with biological tissues. *J R Soc Interface*. 2006;3(11):741–752.
12. Chanda M, Roy SK. *Plastics Technology Handbook*. 4th ed. CRC Press; 2006.
13. Svirskis D, Wright BE, Travas-Sejdic J, Rodgers A, Garg S. Evaluation of physical properties and performance over time of an actuating polypyrrole based drug delivery system. *Sens Actuators B*. 2010;151(1):97–102. doi:10.1016/j.snb.2010.09.042
14. Svirskis D, Sharma M, Yu Y, Garg S. Electrically switchable polypyrrole film for the tunable release of progesterone. *Ther Deliv*. 2013;4(3):307–313. doi:10.4155/tde.12.166
15. Zhao Y-H, Niu C-M, Shi J-Q, Wang -Y-Y, Yang Y-M, Wang H-B. Novel conductive polypyrrole/silk fibroin scaffold for neural tissue repair. *Neural Regen Res*. 2018;13(8):1455–1464. doi:10.4103/1673-5374.235303

16. Chen F, Cai W. Nanomedicine for targeted photothermal cancer therapy: where are we now? *Nanomedicine (Lond)*. 2015;10(1):1–3. doi:10.2217/nnm.14.186
17. Eyvazzadeh N, Shakeri-Zadeh A, Fekrazad R, Amini E, Ghaznavi H, Kamran Kamrava S. Gold-coated magnetic nanoparticle as a nanotheranostic agent for magnetic resonance imaging and photothermal therapy of cancer. *Lasers Med Sci*. 2017;32(7):1469–1477. doi:10.1007/s10103-017-2267-x
18. Mirrahimi M, Abed Z, Beik J, et al. A thermo-responsive alginate nanogel platform co-loaded with gold nanoparticles and cisplatin for combined cancer chemo-photothermal therapy. *Pharmacol Res*. 2019;143:178–185. doi:10.1016/j.phrs.2019.01.005
19. Machida S, Miyata S, Techagumpuch A. Chemical synthesis of highly electrically conductive polypyrrole. *Synth Met*. 1989;31(3):311–318. doi:10.1016/0379-6779(89)90798-4
20. Ansari R. Polypyrrole conducting electroactive polymers: synthesis and stability studies. *E J Chem*. 2006;3(4):186–201. doi:10.1155/2006/860413
21. Theriault A, Wang Q, Gapor A, Adeli K. Effects of γ-tocotrienol on ApoB synthesis, degradation, and secretion in HepG2 cells. *Arterioscler Thromb Vasc Biol*. 1999;19(3):704–712. doi:10.1161/01.ATV.19.3.704
22. Mosmann T. Rapid colorimetric assay for cellular growth and survival: application to proliferation and cytotoxicity assays. *J Immunol Methods*. 1983;65(1):55–63. doi:10.1016/0022-1759(83)90303-4
23. Fadel M, Kassab K, Youssef T, El-Kholy AI. One-step synthesis of phyto-polymer coated gold nanospheres as a delivery system to enhance resveratrol cytotoxicity. *Drug Develop Indus Pharm*. 2019:1–9.
24. Thomas JR, Silverman S, Nelson J. *Research Methods in Physical Activity, 7E: Human Kinetics*. 2015.
25. De Muth JE. *Basic Statistics and Pharmaceutical Statistical Applications*. 3rd ed. CRC Press; 2014.
26. Odian G, Odian UG; Wiley J, Sons, Library WO. *Principles of Polymerization*. Wiley; 2004.
27. Puddephatt RJ. *The Chemistry of Gold*. Elsevier Scientific Pub. Co.; 1978.
28. Armarego WLF. *Purification of Laboratory Chemicals*. Elsevier Science; 2017.
29. Lindqvist I. *Inorganic Adduct Molecules of Oxo-Compounds*. Springer Berlin Heidelberg; 2013.
30. Tan Y, Ghandi K. Kinetics and mechanism of pyrrole chemical polymerization. *Synth Met*. 2013;175:183–191. doi:10.1016/j.synthmet.2013.05.014
31. Song H, Li T, Han Y, Wang Y, Zhang C, Wang Q. Optimizing the polymerization conditions of conductive polypyrrole. *J Photopolymer Sci Technol*. 2016;29(6):803–808. doi:10.2494/photopolymer.29.803
32. Freitas de Freitas L, Varca GHC, Dos Santos Batista JG, Benévolo Lugão A. An overview of the synthesis of gold nanoparticles using radiation technologies. *Nanomaterials (Basel, Switzerland)*. 2018;8(11):939. doi:10.3390/nano8110939
33. Rai M, Duran N. *Metal Nanoparticles in Microbiology*. Berlin Heidelberg: Springer; 2011.
34. Su W-F. Radical chain polymerization. In: Su W-F, editor. *Principles of Polymer Design and Synthesis*. Berlin, Heidelberg: Springer Berlin Heidelberg; 2013:137–183.
35. Gachard E, Remita H, Khatouri J, Keita B, Nadjo L, Belloni J. *Radiation-Induced and Chemical Formation of Gold Clusters*. Vol. 221998.
36. Đurović MD, Puchta R, Bugarčić ŽD, van Eldik R. Studies on the reactions of [AuCl4]−AuCl 4] − with different nucleophiles in aqueous solution. *Dalton TransactionsTrans*. 2014;43(23):8620–8632. doi:10.1039/C4DT00247D
37. Lingane J. *Standard Potentials of Half-Reactions Involving + 1 and + 3 Gold in Chloride Medium: Equilibrium Constant of the Reaction AuCl4− + 2Au + 2Cl− = 3AuCl2−*. Vol 41962.
38. Wuithschick M, Birnbaum A, Witte S, et al. Turkevich in new robes: key questions answered for the most common gold nanoparticle synthesis. *ACS Nano*. 2015;9(7):7052–7071. doi:10.1021/acsnano.5b01579
39. Eisler R. *Eisler's Encyclopedia of Environmentally Hazardous Priority Chemicals*. Elsevier Science; 2007.
40. Fox MA, Whitesell JK. *Organic Chemistry*. Jones and Bartlett Publishers; 2004.
41. Miller FP, Vandome AF, McBrewster J. *Le Chatelier´s Principle: Chemistry, Chemical Equilibrium, Henry Louis Le Chatelier, Karl Ferdinand Braun, Concentration, Temperature, Volume, Pressure, Lenz´s Law, Homeostasis*. Status Quo: Alphascript Publishing; 2009.
42. Myers R. *The Basics of Chemistry*. Greenwood Press; 2003.
43. Mohamad Sadeghi GM, Morshedian J, Barikani M. The effect of initiator-to-monomer ratio on the properties of the polybutadiene-ol synthesized by free radical solution polymerization of 1,3-butadiene. *Polym Int*. 2003;52(7):1083–1087. doi:10.1002/pi.1172
44. Nijenhuis AJ, Grijpma DW, Pennings AJ. Lewis acid catalyzed polymerization of L-lactide. Kinetics and mechanism of the bulk polymerization. *Macromolecules*. 1992;25(24):6419–6424.
45. Kricheldorf HR, Nuyken O, Swift G. *Handbook of Polymer Synthesis:*. 2nd ed. CRC Press; 2004.
46. Alkire RC, Gerischer H, Kolb DM, Tobias CW. *Advances in Electrochemical Science and Engineering*. Wiley; 2008.
47. Ahmad T, Wani IA, Ahmed J, Al-Hartomy OA. Effect of gold ion concentration on size and properties of gold nanoparticles in TritonX-100 based inverse microemulsions. *Appl Nanosci*. 2014;4(4):491–498. doi:10.1007/s13204-013-0224-y
48. Suchomel P, Kvitek L, Prucek R, et al. Simple size-controlled synthesis of Au nanoparticles and their size-dependent catalytic activity. *Sci Rep*. 2018;8(1):4589. doi:10.1038/s41598-018-22976-5
49. Kim H-S, Seo YS, Kim K, Han JW, Park Y, Cho S. Concentration effect of reducing agents on green synthesis of gold nanoparticles: size, morphology, and growth mechanism. *Nanoscale Res Lett*. 2016;11(1):230. doi:10.1186/s11671-016-1393-x
50. Mühlig S, Rockstuhl C, Yannopapas V, Bürgi T, Shalkevich N, Lederer F. Optical properties of a fabricated self-assembled bottom-up bulk metamaterial. *Opt Express*. 2011;19(10):9607–9616. doi:10.1364/OE.19.009607
51. Cui W, Lu W, Zhang Y, Lin G, Wei T, Jiang L. Gold nanoparticle ink suitable for electric-conductive pattern fabrication using in ink-jet printing technology. *Colloids Surf A*. 2010;358:35–41. doi:10.1016/j.colsurfa.2010.01.023
52. nauk Raaa. *Polymer Science*. MAIK Nauka/Interperiodica Pub; 2003.
53. Bhattacharjee S. In relation to the following article "DLS and zeta potential - What they are and what they are not? *J Control Release*. 2016;235:337–351. doi:10.1016/j.jconrel.2016.07.002
54. Ramanujam BTS, Annamalai PK. 1 - Conducting polymer–graphite binary and hybrid composites: structure, properties, and applications. In: Thakur VK, Thakur MK, Pappu A, editors. *Hybrid Polymer Composite Materials*. Woodhead Publishing; 2017:1–34.